The International Journal of Advanced Manufacturing Technology (2018) 95:2989–2999
https://doi.org/10.1007/s00170-017-1444-1

ORIGINAL ARTICLE

Effect of cryogenic treatment on the microstructure and the wear behavior of WC-Co end mills for machining of Ti6Al4V titanium alloy

Osman Nuri Celik[1] · Abdullah Sert[1] · Hakan Gasan[2] · Mustafa Ulutan[1]

Received: 20 July 2017 / Accepted: 27 November 2017 / Published online: 2 December 2017

Abstract

This paper compares some of the key machinability aspects acquired during milling of Ti6Al4V titanium alloy with uncoated and coated cryogenically treated end mills. Tool wear, coefficient of friction, cutting force, and chip morphology were the major criteria considered. Ti6Al4V is one of the titanium alloys that are widely used in aerospace and biomedical applications; however, it has a poor machinability and tribological properties. To evaluate the performance of cryogenically treated end mills, milling operations using a force dynamometer and dry sliding tests were conducted. The milling operations were conducted with a cutting speed of 90 m/min, a feed rate of 0.11 mm/tooth, a 1-mm axial depth of cut, and a 10-mm radial depth of cut under dry cutting conditions. The dry sliding tests were conducted using a tribometer with a ball-on-disk geometry under 10 N load and a speed of 5 cm/s. The milling test results showed that flank wear, chipping, and tool breakage were the wear mechanisms of the end mills. The cutting force measurements and the dry sliding tests showed that the cutting force and friction force values decreased when the cryogenic treatment time increased. As a result of the study, tools treated cryogenically for 36 h showed the best performance for the cutting force, friction force, and tool wear criteria. These improvements were characterized with hardness, fracture toughness, scanning electron microscope (SEM), energy-dispersive spectroscopy (EDS), and X-ray diffraction (XRD) analyses.

Keywords WC-Co · Cryogenic treatment · Ti6Al4V · Tool wear · Cutting force · Friction force

1 Introduction

Tool life plays a critical role in increasing productivity in the machining industry and thus has important economic value. To increase tool life, a widely used method is heat treatment; for example, Khan and Ahmed [1] used cryogenic cooling, and Zhang et al. [2] applied cryogenic treatment to cutting tool materials for the machining process. Ti6Al4V titanium alloy is widely used in aerospace and biomedical applications (and it accounts for more than 50% of all titanium alloys) because of its good strength-to-weight ratio under high temperature and its high corrosion resistance [3–5]. However, Ti6Al4V titanium alloy is a difficult-to-machine material because of its low Young's modulus, high chemical affinity, and low thermal conductivity [6–9]. For machining of Ti6Al4V titanium alloy, cutting tools with sharp cutting edges must be used, and some properties, such as high wear resistance and hot hardness, must be improved.

Kalyan Kumar and Choudhury [10] and Podgornik et al. [11] have determined that cryogenic treatment is one of the treatment methods that can improve cutting tool properties, such as the wear resistance, fracture toughness, and tool life their materials. Senthilkumar et al. [12] indicated that the residual stresses were increased by the cryogenic treatment method. In addition, they determined that the toughness of the material was not significantly influenced by cryogenically treated samples with respect to conventional heat-treated samples.

By using the cryogenic treatment on Fe-based alloys, the transformation of the retained austenite to martensite and the formation of fine carbide particles occurred. Das et al. [13] used cryogenic treatment on AISI D2 tool steel for different treatment times (0, 12, 36, 60, and 84 h) to find the optimum

✉ Osman Nuri Celik
oncelik@ogu.edu.tr

[1] Mechanical Engineering Department, Engineering & Architecture Faculty, Eskisehir Osmangazi University, 26480 Eskisehir, Turkey

[2] Metallurgical and Materials Department, Engineering & Architecture Faculty, Eskisehir Osmangazi University, Eskisehir, Turkey

treatment time for obtaining the maximum wear resistance. A pin-on-disk test machine was used to determine the optimum wear resistance. They found that the 36-h cryogenic treatment was the best treatment time. The wear resistance of AISI D2 tool steel cryogenically treated for 36 h was 76.2 times higher than that of a conventionally treated tool. Amini et al. [14] investigated the effects of different treatment times (24, 36, 48, 72, 96 and 120 h) on the mechanical and microstructural changes of AISI D3 tool steel. They found that the optimum treatment time was 36 h for obtaining the higher hardness and carbide percentage values.

According to the findings of Gill et al. [15], by using the cryogenic treatment on cemented carbides, the following occurred: the formation of fine carbides (M_6C type: Co_3W_3C and $M_{12}C$ type: Co_6W_6C), the development of a homogeneous distribution of carbide particles and the change of residual stress and cobalt phase transformation (α-Co to ε-Co). Özbek et al. [16] studied the cryogenic treatment of different holding times (12, 24, 36, 48, and 60 h) of tungsten carbide inserts to reduce tool wear. Co_6W_6C carbide precipitation was found on the 12- and 24-h treated samples according to the XRD profiles. Because of the cryogenic treatment, the wear resistances of the inserts were improved up to 29% in flank wear, and the 24-h cryogenically treated samples showed the best wear resistance. Yong and Ding [17] investigated the effect of cryogenic treatment on WC-Co inserts with different holding times (2, 4, 8, 24, and 72 h). The wear resistances of cryogenically treated samples were higher than those of untreated samples. They found that improvement of the mechanical properties of cryogenically treated samples was achieved by the mechanism of residual compression stress and phase transformation of cobalt. Gill et al. [18] implemented the cryogenic treatment at temperatures of − 110 and − 196 °C on TiAlN-coated tungsten carbide inserts and found that the enhancement of tool life was 25.53% for inserts treated at the temperature of − 110 °C compared to untreated inserts. In addition, they determined that the cryogenic treatment at the temperature of − 196 °C weakens the adhesion bonding of the coating. Thakur et al. [19] investigated the effect of post-treatments on the performance of tungsten carbide insert during the turning of Inconel 718. They found that the wear resistance of cryogenically treated inserts was improved and that the cutting force values of cryogenically treated inserts were lower than those of untreated inserts.

Few studies are available in the literature on the cutting performance of cryogenically treated cutting end mills on the milling of Ti6Al4V under dry cutting conditions. This study aimed to investigate the effect of cryogenic treatment of coated and uncoated end mills on the milling performance and determine the optimal condition in face milling of Ti6Al4V titanium alloy. The mechanical and tribological behaviors of the cryogenically treated tools are also studied via cutting force and friction force.

2 Experimental procedure

Face milling tests were performed via a Makino GT8 milling center with a maximum speed of 5000 rpm. The samples used in the milling operation were Ti6Al4V titanium alloy blocks and tungsten carbide end mills with 325 and 1546 HV microhardness, respectively. A schematic drawing of the Ti6Al4V blocks (6.08 Al, 3.89 V, 0.17 Fe, 0.02 C, 0.001 H, 0.02 N, 0.06 O and balance Ti), tungsten carbide end mills (WC-10%Co), and the up-milling process with dimensions are shown in Fig. 1.

Two types of coated (AlCrN and AlTiN) and uncoated WC-10% Co carbide tools with four flutes were used in the experiments. For the milling tests, three types of end mills were cryogenically treated at a temperature of − 196 °C for 12 h (CT12), 24 h (CT24), and 36 h (CT36) using a programmable cryogenic system. For comparison with the treated samples, one group of end mills was not cryogenically treated (CT00).

The milling tests were conducted by dry cutting at a cutting speed (V_c) of 90 m/min, a feed rate (F_z) = 0.11 mm/tooth, and depth of cut (DOC) = 1 mm. The cutting forces were measured with a Kistler 9257BA stationary dynamometer mounted under the workpiece (Fig. 2). The three-axis force signals were acquired by Dynoware software. The total cutting force (F_T) was obtained according to the following equation:

$$F_T = \sqrt{F_x^2 + F_y^2 + F_z^2} \ [\mathrm{N}] \tag{1}$$

The wear properties of WC-10% Co end mills were characterized by using the dry sliding ball-on-disk test. Before the dry sliding tests and SEM examinations, the samples were cleaned for 30 min in an ultrasonic cleaner using acetone and ethanol. Dry sliding tests were performed using a CSM tribometer with a ball-on-disk geometry. The balls (3 mm in diameter) used in the experiment were made of WC-6% Co. The tribological tests were conducted in an air-conditioned environment (25 ± 2 °C temperature and 30 ± 2% relative humidity) under a load of 10 N at a speed of 5 cm/s and over a

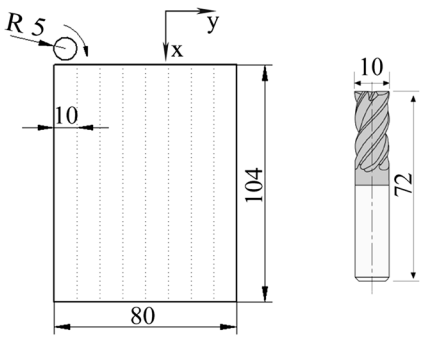

Fig. 1 Up milling with the dimensions of the materials

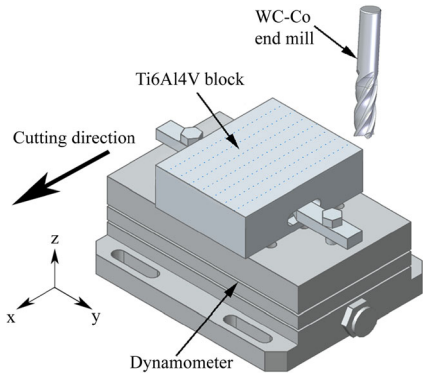

Fig. 2 Schematic drawing of the Kistler dynamometer during milling operation

total sliding distance of 1 km. The prepared disks from the end mills were polished with 1-μm diamond suspension, and their surface roughnesses (all samples $R_a = 0.02$ μm) were measured using a Mitituyo SJ-400 surface profilometer to minimize the effect of asperities on the wear tests. The friction force and the coefficient of friction (COF) values of the samples were obtained via the tribometer during the tests.

The microhardness values were measured with 30 kg loads according to the ISO 3878 standards (FV800, Future Tech). The fracture toughness $K_{IC(30\ kg)}$ was obtained via the Palmqvist method, which uses the corner crack length of a Vickers hardness indentation (Fig. 3). The following equation was applied to determine the K_{IC} values:

$$K_{IC} = 0.0028\sqrt{H_V\left(\frac{P}{\sum l}\right)}\ \left[\mathrm{MNm}^{-3/2}\right] \quad (2)$$

where H_V is the Vickers hardness, P is the applied load (N), and l is the crack length (mm).

A Zeiss-Supra 50VP scanning electron microscope was used to observe the wear mechanisms and the microstructure of the WC-Co end mills. An EDS was used for elemental analysis of the materials. The phase compositions of cryogenically treated and untreated WC-Co end mills were determined using an X-ray diffractometer (PANalytical—Empyrean) with Cu Kα radiation. To avoid WC phase diffraction peak interference to Co phase in X-ray diffraction analysis, the WC-Co tungsten carbide was electrolytically etched in a solution containing NaOH and $K_3Fe(CN)_6$ at 4 V and 0 °C.

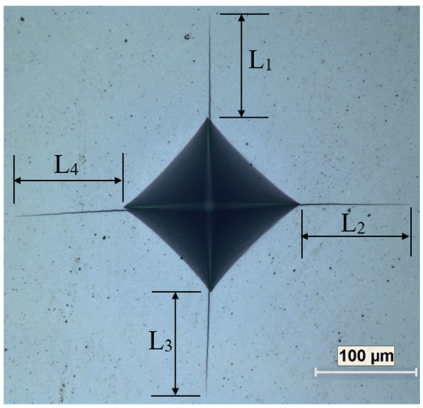

Fig. 3 Diagram of the cracking system obtained using the Vickers hardness test-Palmsqvit method

3 Results and discussions

3.1 Microstructure and phase analysis of end mills

Cemented carbides have three main phases in the microstructure: α phase (tungsten carbide), β phase (cobalt binder), and η phase (multiple carbides of tungsten and binder). An SEM image of tungsten carbide is shown in Fig. 4. As shown in the figure, the light gray WC particles are surrounded by dark Co binder phase, and no η phases were observed after cryogenic treatment, as indicated in references [20, 21]. When the W-Co-C equilibrium diagram is examined, the element of C must have a composition of approximately 5.4% or less for the eta phase to form in the structure because the eta phase does not occur if this ratio is exceeded. In addition, the formation of eta phases is avoided because the eta phases are so brittle [20]. Accordingly, the presence of the eta phase in the construction will negatively affect the life of the cutting tools. Figure 5 shows EDS analysis of the CT00 sample; the W, Co, and C amounts are 84.34, 10.13, and 5.53 wt%, respectively.

XRD patterns of the samples are marked in terms of different cryogenic treatment conditions in Fig. 6a, b. In the XRD results, each cryogenic treatment results in identical peak positions, with the intensity of the peaks varying depending on the cryogenic treatment time, as shown in Fig. 6b. After selective electrolytical etching, the peaks of the WC phase were corroded to explore the binder phase. It is known that the crystal structure of Co is fcc (α-Co) at a temperature higher than 417 °C; at a temperature below 417 °C, the crystal structure is hcp (ε-Co), and cobalt phase transformation (α-Co to ε-Co) occurs by using cryogenic treatment to WC-Co end mills [2]. The amounts of the Co phase in all of the samples

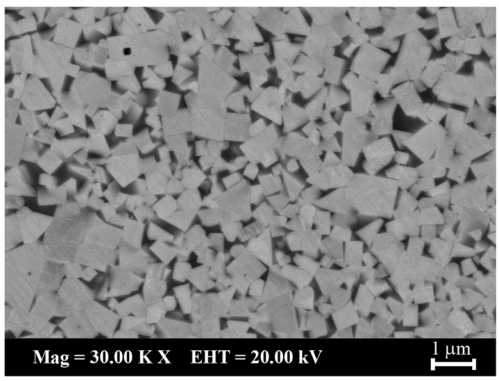

Fig. 4 SEM image of CT00

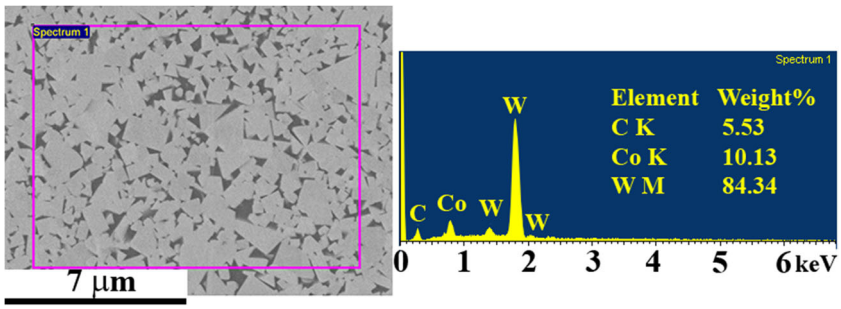

Fig. 5 EDS analysis of cemented carbide (10% Co)

cryogenically treated at different times were determined by Rietveld analysis. The amounts of the Co phase in the cryogenically treated and untreated samples are shown in Table 1. It is seen that after cryogenic treatment of WC-Co end mills, the amount of ε-Co is increased. Thus, it is concluded that cryogenic treatment affects the allotropic transformation of Co.

3.2 Mechanical properties

The microhardness and fracture toughness measurements of the untreated and cryogenically treated samples are shown in Fig. 7. There were no significant changes in the hardness values of all the samples. The fracture toughness values of the CT12 and CT24 samples were higher than that of the CT00 sample by 4 and 5%, respectively. When analyzing the CT36 sample, the values of hardness and fracture toughness were almost the same as that of the CT00 sample. It was seen that the hardness values were slightly increasing with increasing cryogenic treatment time. Yong and Ding [17] determined that the hardness and fracture toughness values of tungsten carbide tools were not affected significantly by cryogenic treatment. They reported that the hardness values of 24-h and 72-h cryogenically treated tools increased approximately 2.4%. Vadivel and Rudramoorthy [22] stated that the toughness of cutting tools was not significantly affected by cryogenic treatment. Gill et al. [23] applied cryogenic treatment on the tungsten carbide inserts; the hardness was improved by only approximately 5%. Previous studies have shown that there is no significant change in hardness and toughness values. This observation can be explained as follows: the grain size or shape does not change in the microstructure by cryogenic treatment. Saito et al. [24] stated that the factors for determining the hardness of the sintered carbides are the size, the distribution of WC particles, and the amount of Co. After the cryogenic process, some alpha phase in the Co structure is transformed into the epsilon phase. Thus, the change in the hardness and fracture toughness values with cryogenic treatment found in this study is in agreement with the literature.

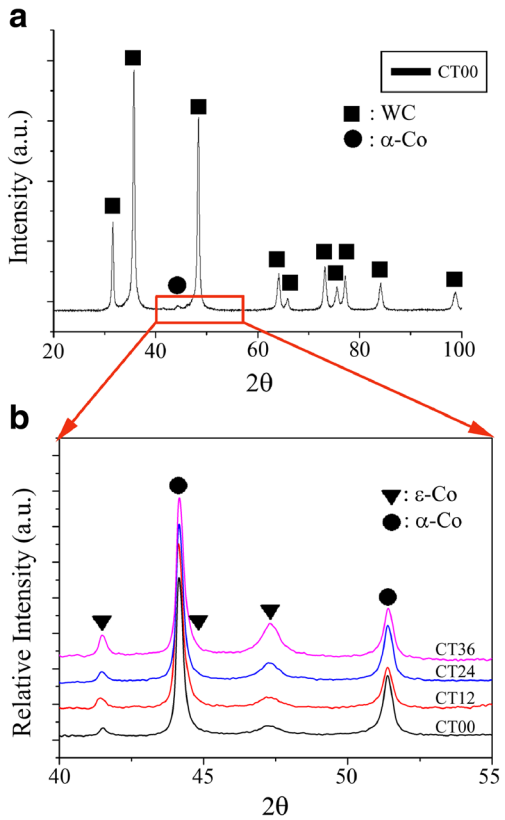

Fig. 6 XRD patterns of samples. **a** Before electrolytical etching. **b** After electrolytical etching

3.3 Sliding wear properties

The friction forces of cryogenically treated and untreated samples are given as a function of sliding distance for a 5-cm/s sliding speed under a contact load of 5 N, as shown in Fig. 8. The curves show some stages with fluctuations. In the first stage, the friction force values were increased for

Table 1 Rietveld analysis results (wt%) for the samples

Sample	Phase	
	α-Co (fcc)	ε-Co (hcp)
CT00	85.91	14.09
CT12	81.12	18.88
CT24	73.49	26.51
CT36	66.04	33.96

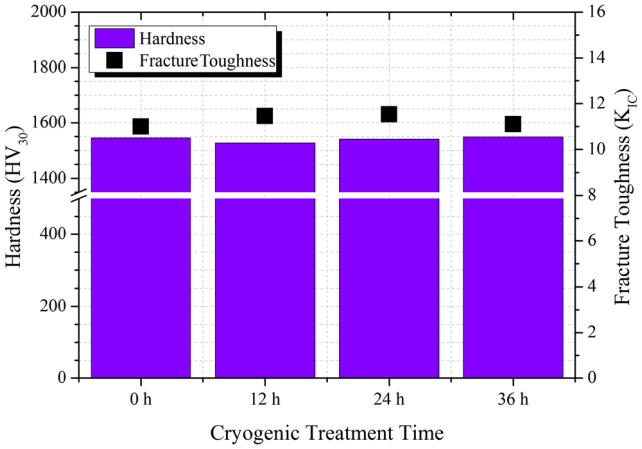

Fig. 7 Hardness and fracture toughness values of end mills

approximately 15 m sliding distance, and then, the values were decreased. This is related to a mechanical polishing effect between asperities of the counter surface [25]. At the beginning of the sliding tests, the asperities of surfaces were touching each other to inhibit sliding motion. During the tests, the asperities of the surfaces were crushed under the load; thus, the friction force values and the surface roughness were reduced in the second stage (15–250 m). In the third stage (after 250 m), some fluctuations were observed with different sizes because of the hard WC debris from the contact surfaces and asperities. Kagnaya et al. [26] explained these fluctuations as being caused by the debris acting as a third body in the contact surfaces during sliding motion. In this case, the resistance of friction may occur and increase the instantaneous coefficient of friction.

As shown in Fig. 8, the COF and the friction force values are changed by the cryogenic treatment. Increasing the cryogenic treatment time from 12 to 36 h, cobalt phase transformation (α-Co to ε-Co) occurred, thereby improving the coefficient of friction and the friction force values; this

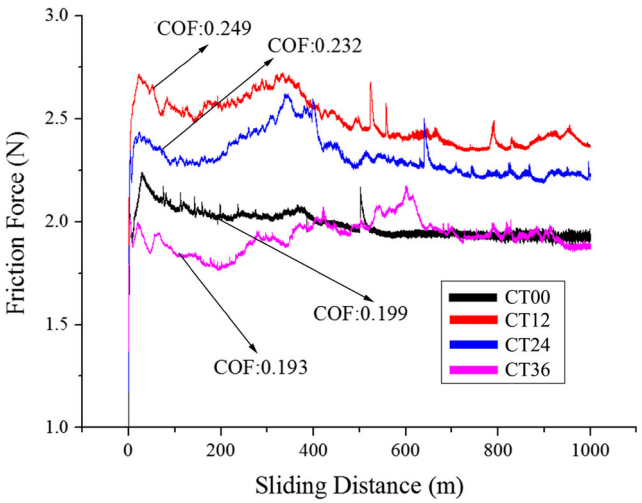

Fig. 8 COF and friction force values of samples

improvement is related to the Co phase crystal structure. Mezenes et al. [27] explained that metals with a hexagonal crystal structure have a limited number of slip systems compared to those with a face-centered cubic structure. Friction depends on how easily a material can undergo plastic deformation; thus, metals with a hexagonal crystal structure have lower friction coefficients than face-centered cubic and body-centered cubic metals. The lowest values of the COF and the friction force were found in the CT36 sample. It is also seen that there were not many fluctuations in the curve of the CT00 sample compared to the other curves. It is considered that the cryogenic treatment affected the crystal structure of the samples and perhaps caused the formation of ε-Co. The debris might be affected by new formations, resulting in the observed fluctuations.

3.4 Cutting performance

The milling tests were performed using the coated and uncoated tools at a 90-m/min cutting speed and a 0.11-mm/tooth feed rate. The graphs are plotted in Fig. 9 based on the data recorded by a stationary dynamometer for multiple passes of the milling process. Each group of peaks indicates a cutting force value corresponding to a single pass of the cutting tool. The cutting forces in the F_x, F_y, and F_z directions are shown in Fig. 9. Note that the dominant cutting force is F_x because the F_x values increased during the number of passes in the milling tests, whereas the F_y and F_z values exhibited almost identical trends.

The cutting forces of the coated and uncoated tools with different cryogenic treatment times are shown in Fig. 9 and Table 2. Data for the conditions of uncoated tools with 12, 24, and 36 h of cryogenic treatments are shown in Fig. 9a–c, respectively. The F_y and F_z cutting force values show an almost identical trend with the number of cutting passes for all conditions. However, the Fx values are found to vary according to the number of cutting passes. The variation of the peak forces could be attributed to the tool wear, the work-hardened material, and the thermal effects of the tool-workpiece interface [28]. This tendency is explained by Khanna and Davim [29] as follows: the machining becomes highly adiabatic for titanium alloys because of their low thermal conductivity, and the heat-generated zone cannot be carried away during the very short interval of time during which the material passes through this zone. At the beginning of the first cutting pass, the cutting edge of the tool was sharp, and the cutting force values fluctuated over a very small range. In the next cutting pass, the fluctuation of the cutting force values increased because of the tool wear, in agreement with the results of Zhang et al. [30]. During the milling tests of Ti6Al4V titanium alloy with end mills, the cutting edges of the tool lost their sharpness, and a higher friction coefficient and larger contact area of the tool/workpiece interfaces are generated [31]. As a result,

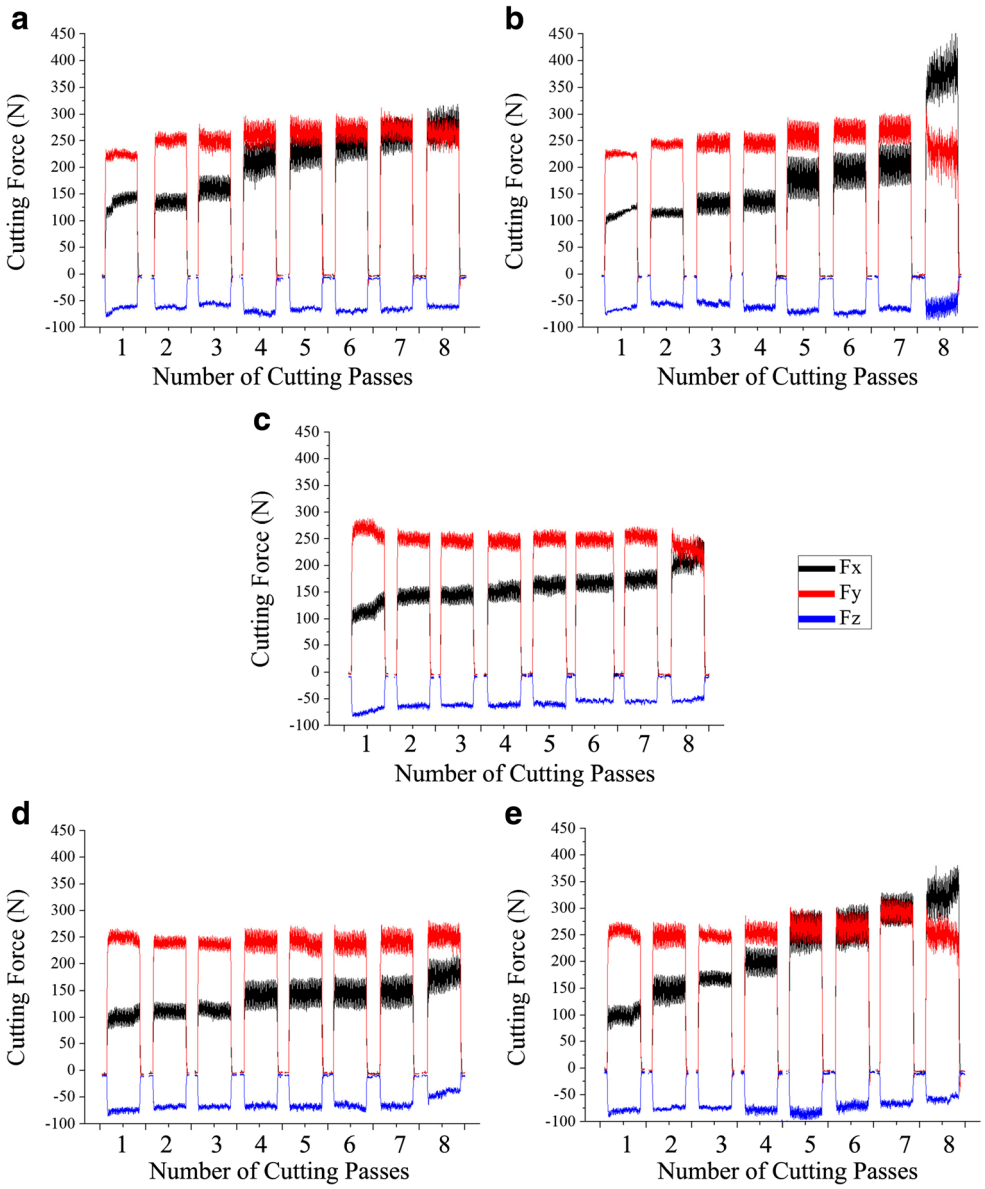

Fig. 9 The cutting forces of different tools. **a** CT12-uncoated. **b** CT24-uncoated. **c** CT36-uncoated. **d** CT36-AlCrN. **e** CT36-AlTiN

Table 2 Different test values of the cutting tools

Samples	Cryogenic treatment (− 196 °C) Time (h)	Cutting parameters			Coefficient of friction	Average values of cutting force (N)	Notch wear (μm)
		Cutting speed (m/min)	Feed rate (mm/tooth)	Depth of cut (mm)			
CT12-uncoated	12	90	0.11	1	0.249	339.9	116.1
CT12-AlCrN	12	90	0.11	1	–	315.6	83.0
CT12-AlTiN	12	90	0.11	1	–	317.8	185.3
CT24-uncoated	24	90	0.11	1	0.232	327.4	164.7
CT24-AlCrN	24	90	0.11	1	–	300.1	87.2
CT24-AlTiN	24	90	0.11	1	–	302.3	110.1
CT36-uncoated	36	90	0.11	1	0.193	306.5	66.2
CT36-AlCrN	36	90	0.11	1	–	291.1	46.4
CT36-AlTiN	36	90	0.11	1	–	354.4	154.0

the cutting forces obtained are greater. The cutting force amplitudes increased in the 12- and 24-h cryogenically treated samples at the fourth pass and fifth pass, respectively. It was considered that the serious variations in the cutting force amplitude in the 12- and 24-h cryogenically treated samples at the fourth and fifth passes were related to tool cutting edge breakage or dulling of the cutting tool. Alternatively, the amplitude of cutting force of the 36-h cryogenically treated sample was found to be more stable and lower than those of the 12-h and 24-h cryogenically treated samples. From Fig. 9d, e, the cutting force of the CT36-AlCrN sample was found to be more stable and lower than that of the CT36-AlTiN sample. A previous study [32] revealed that the vibration increases the fluctuations of cutting force in milling, resulting in cutting tool edge microchipping and thus reduced tool life. To achieve long tool life for productive milling operation on Ti6Al4V alloy and to prevent cutting edge breakage, the vibration/cutting force of the tool should be kept lower.

The average values of all total cutting forces are given in Table 2. It was seen that increasing the cryogenic treatment times from 12 to 36 h positively affected the coated and uncoated tools, except the situation of the CT36-AlTiN sample. For this situation, it was considered that the AlTiN coating was adversely affected by the 36-h cryogenic treatment. In the study of the cryogenic treatment of TiAlN-coated cutting tools, Gill et al. [18] reported that the coating-substrate interfacial adhesion bond was weakened by the cryogenic treatment (at −196 °C with 38 h) via the materials with different coefficients of expansion, resulting in degraded cutting performance of the cryogenically treated cutting tools. Nouari and Makich [33] stated that, for the same cutting conditions, the cutting forces obtained with the coated tool when machining Ti alloy are smaller than those obtained with the uncoated tools. However, in this study, the CT36-uncoated tool shows smaller cutting force values than the CT12-AlCrN-, CT12AlTiN-, and CT36-AlTiN-coated tools, likely because 36-h cryogenically treated uncoated cutting tools are comparable to coated tools. It was also considered that the friction force and the COF values obtained by the sliding tests and the cutting force obtained by the milling tests were affected similarly by the cryogenic treatment, particularly for the uncoated tools. While increasing the cryogenic treatment time from 12 h to 36 h, the cutting force, friction force, and COF values decreased. It could be said that the friction force and COF values are related to the cutting force, and if the friction force and COF values are decreased, then the cutting force will be decreased.

3.5 Chip formation

In milling operations, chip formation plays an important role in terms of the surface finish and the tool life. Chip formation is dependent on the factors (such as the tool geometry, the milling parameters, the hardness of the workpiece and the machining environment) that affect the surface quality [34]. Figure 10 depicts the chip macro-images obtained after the last pass of different cryogenically treated and coated-uncoated tools. No significant difference was seen in the chip morphology with changes in the cryogenic treatment time and different coating conditions. However, there was a noteworthy change in the chip morphology in the CT24-uncoated tool (Fig. 10b) and the CT36-AlTiN coated tool (Fig. 10e). After machining with these tools, some chips were found to be longer and more twisted than the chips of the other conditions. The reason for the longer chips was believed to be the very high friction that led to the increased heat generation when cutting the material, and the chips were adhered each other. Figure 9b–e shows that in the last pass, the amplitudes of the cutting forces were higher and were not stable because of the adhered chips. Strano et al. [35] observed a transition from a

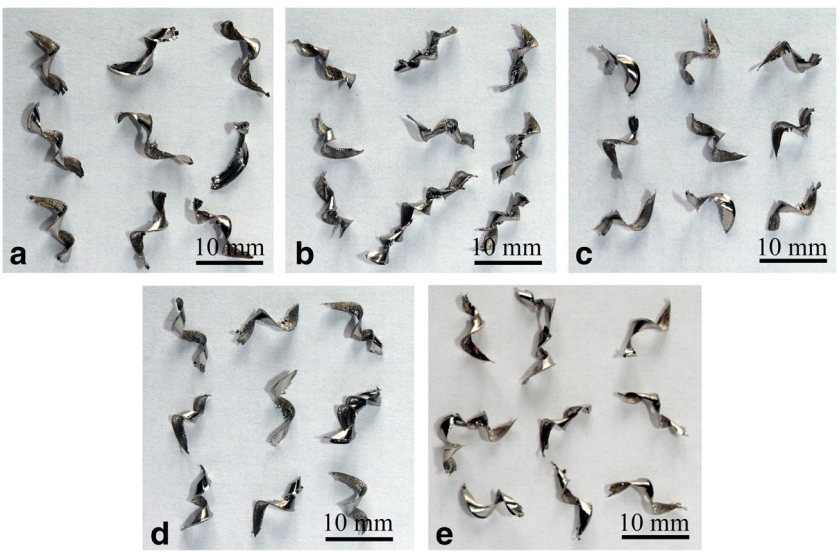

Fig. 10 Chip morphologies (after machining eight passes) of cutting tools. **a** CT12-uncoated. **b** CT24-uncoated. **c** CT36-uncoated. **d** CT36-AlCrN coated. **e** CT36-AlTiN coated

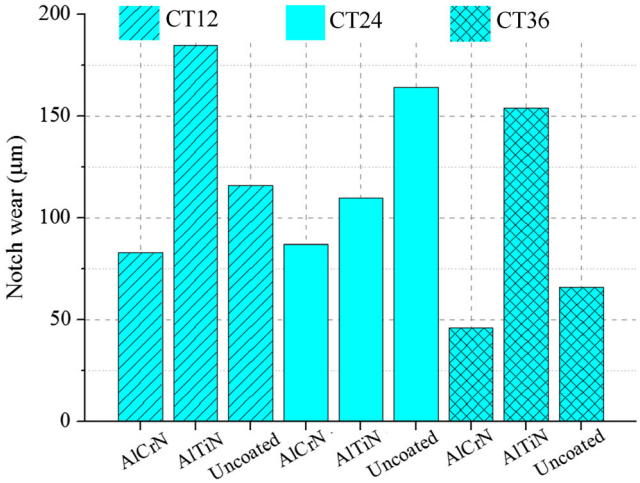

Fig. 11 Depth of notch wear of the cutting tools

short helical chip to a twisted type when machining Ti6Al4V alloy with the increase in tool wear. CT36-uncoated (Fig. 10c) and CT36-AlCrN (Fig. 10d) tools showed smaller chips because, for the given conditions, the CT36-AlCrN- and CT36-uncoated tools showed better wear performance and average values for the cutting forces. In a recent study, Mo et al. [36] stated that AlCrN coatings showed better friction and wear properties than AlTiN coatings. Thus, it is possible to conclude that CT36-AlCrN- and CT36-uncoated tools showed lower coefficients of friction, and this lower friction may affect the chip morphology and wear properties.

3.6 Tool wear examination

Non-uniform wear at the flank face was found under severe cutting conditions. In almost all cutting conditions, the tool failed by notch wear at the location of the DOC line, thus affecting the tool life. In addition to wear mechanisms, flank wear, tool breakage, chipping, and built-up edges (BUE) formation were revealed in the SEM images. The depth of notch wear was used in the determination of the tool life because notch wear was the dominant tool failure mode.

Figure 11 and Table 2 (numerical values of tests data) show the change in notch wear for different cryogenic treatment times and coated-uncoated conditions after the eighth pass of machining. It was seen that AlCrN coating showed better notch wear resistance in all samples with different cryogenic treatment times. The best result for the notch wear resistance was seen in the case of 36 h of cryogenic treatment time with AlCrN coating; in addition, the uncoated tool for the same cryogenic treatment time showed the next best result. It could be seen that the uncoated tool with 36 h of cryogenic treatment showed better performance than the 12- and 24-h cryogenically treated and coated tools and the 36-h cryogenically treated AlTiN tool.

During end milling, the tool life depends on chipping, cracks, and breakage of the cutting edge rather than other cutting process, such as turning and drilling, because the tool cutting edge enters and exits from the workpiece several times during the milling operation [37]. Wang et al. [38] stated that the residual stress of the coating, mechanical impact, thermal stress, and fatigue cracks affects the peeling of the coating and that the peeled coating initiated the breakage mechanism of coated carbide tools. In Fig. 12, notch wear could be seen near the DOC line, and the BUE was observed at the lower part of the notch wear.

In the machining of titanium alloy, because of the low thermal conductivity and the high temperature between the chip and the cutting edge, the chips adhered to the cutting

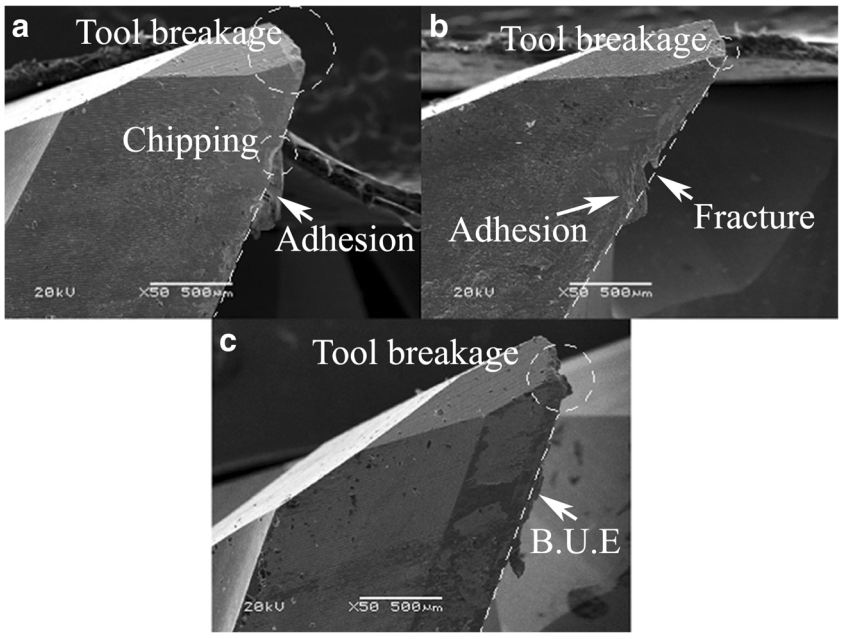

Fig. 12 SEM images of cutting tools. **a** CT36-AlCrN. **b** CT36-AlTiN. **c** CT36-uncoated

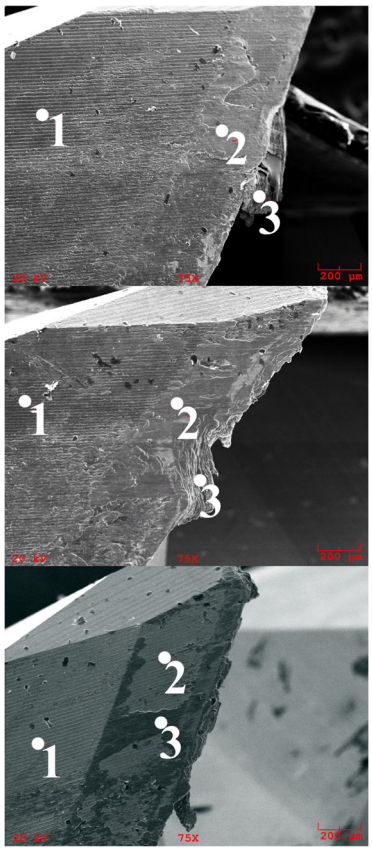

Point 1		Point 2		Point 3	
V	0.989	V	1.553	V	2.103
Ti	10.398	Ti	68.744	Ti	81.804
Al	28.057	Al	8.604	Al	6.657
Co	0.802	Co	0.029	Co	0.504
C	3.307	C	4.836	C	1.257
W	11.836	W	4.582	W	7.675
Cr	27.199	Cr	0.373	Cr	0.000
N	17.412	N	11.279	N	0.000

Point 1		Point 2		Point 3	
V	1.855	V	4.224	V	3.465
Ti	4.696	Ti	2.954	Ti	75.226
Al	2.025	Al	1.725	Al	5.490
Co	8.855	Co	7.272	Co	1.109
C	0.000	C	0.000	C	0.000
W	73.370	W	83.825	W	14.710
N	9.199	N	0.000	N	0.000

Point 1		Point 2		Point 3	
V	3.475	V	1.588	V	0.836
Ti	3.062	Ti	19.286	Ti	59.392
Al	2.993	Al	2.928	Al	3.423
Co	8.796	Co	7.301	Co	3.116
C	0.000	C	0.000	C	0.000
W	81.673	W	68.896	W	33.234

Fig. 13 EDS analysis of the cutting tools. **a** CT36-AlCrN. **b** CT36-AlTiN. **c** CT36-uncoated

edge easily, and the interface of the tool and chip was welded, as shown in Fig. 12. The EDS analysis of the worn tools is shown in Fig. 13. It was also seen that the adhesion and the BUE formation occurred in the cutting edge of the tool. Kasim et al. [39] stated that the maximum chip thickness formed near the DOC line. At this location, the BUE occurred because of the stress on the cutting edge. As a result of the break-off, the BUE suffered from the pitting problem. The chipping was formed by pitting, and the chipping and abrasive wear increased the notch wear.

4 Conclusions

In this research, the effects of cryogenic treatment time on the wear behavior and the cutting performance of WC-Co tungsten carbide tools in face milling of Ti6Al4V titanium alloy were investigated. The results can be summarized as follows:

- XRD results revealed that amount of ε-Co increased after cryogenic treatment.
- The hardness and the fracture toughness values of tungsten carbide tools were not significantly affected by the cryogenic treatment.
- By increasing the cryogenic treatment time from 12 to 36 h, the cobalt phase transformation (α-Co to ε-Co) occurred, thereby improving the coefficient of friction and the friction force values. In addition, the cutting force values of uncoated tools decreased when the cryogenic treatment time increased.
- Flank wear, chipping, built-up edge, and tool breakage are the main wear mechanisms during machining of Ti6Al4V.
- Based on examination of cryogenic heat-treated cutting tools, the uncoated cutting tools were found to provide comparable improvement to that of the coated tools.
- The best results against notch wear and cutting force from the performance tests were obtained on the CT36-AlCrN (36 h) tool.

Acknowledgements The authors would like to acknowledge the support of the Alp Aviation Company for their collaborative work and MMD Ltd. (http://www.mmdtekno.com) performing the cryogenic treatments.

Funding information This work was supported by the Scientific Research Council of Eskisehir Osmangazi University (Grant No: 201515001) and the Scientific and Technological Research Council of Turkey (TÜBİTAK-2211D).

References

1. Khan AA, Ahmed MI (2008) Improving tool life using cryogenic cooling. J Mater Process Technol 196(1–3):149–154. https://doi.org/10.1016/j.jmatprotec.2007.05.030

2. Zhang H, Chen L, Sun J, Wang W, Wang Q (2015) An investigation of cobalt phase structure in WC–Co cemented carbides before and after deep cryogenic treatment. Int J Refract Met Hard Mater 51: 201–206. https://doi.org/10.1016/j.ijrmhm.2015.04.007
3. Arrazola PJ, Garay A, Iriarte LM, Armendia M, Marya S, Le Maître F (2009) Machinability of titanium alloys (Ti6Al4V and Ti555.3). J Mater Process Technol 209(5):2223–2230. https://doi.org/10.1016/j.jmatprotec.2008.06.020
4. Liang L, Liu X, Li X-q, Li Y-Y (2015) Wear mechanisms of WC–10Ni3Al carbide tool in dry turning of Ti6Al4V. Int J Refract Met Hard Mater 48:272–285. https://doi.org/10.1016/j.ijrmhm.2014.09.019
5. Lauro CH, Ribeiro Filho SLM, Brandão LC, Davim JP (2016) Analysis of behaviour biocompatible titanium alloy (Ti-6Al-7Nb) in the micro-cutting. Measurement 93:529–540. https://doi.org/10.1016/j.measurement.2016.07.059
6. Armendia M, Garay A, Iriarte LM, Arrazola PJ (2010) Comparison of the machinabilities of Ti6Al4V and TIMETAL® 54M using uncoated WC–co tools. J Mater Process Technol 210(2):197–203. https://doi.org/10.1016/j.jmatprotec.2009.08.026
7. Sun S, Brandt M, Palanisamy S, Dargusch MS (2015) Effect of cryogenic compressed air on the evolution of cutting force and tool wear during machining of Ti–6Al–4V alloy. J Mater Process Technol 221:243–254. https://doi.org/10.1016/j.jmatprotec.2015.02.017
8. Veiga C, Davim JP, Loureiro AJR (2013) Review on machinability of titanium alloys: the process perspective. Rev Adv Mater Sci 34: 148–164
9. Veiga C, Davim JP, Loureiro AJR (2012) Properties and applications of titanium alloys:A Brief Review. Rev Adv Mater Sci 32: 133–148
10. Kalyan Kumar KVBS, Choudhury SK (2008) Investigation of tool wear and cutting force in cryogenic machining using design of experiments. J Mater Process Technol 203(1–3):95–101. https://doi.org/10.1016/j.jmatprotec.2007.10.036
11. Podgornik B, Paulin I, Zajec B, Jacobson S, Leskovšek V (2016) Deep cryogenic treatment of tool steels. J Mater Process Technol 229:398–406. https://doi.org/10.1016/j.jmatprotec.2015.09.045
12. Senthilkumar D, Rajendran I, Pellizzari M, Siiriainen J (2011) Influence of shallow and deep cryogenic treatment on the residual state of stress of 4140 steel. J Mater Process Technol 211(3):396–401. https://doi.org/10.1016/j.jmatprotec.2010.10.018
13. Das D, Dutta AK, Ray KK (2009) Influence of varied cryotreatment on the wear behavior of AISI D2 steel. Wear 266(1–2):297–309. https://doi.org/10.1016/j.wear.2008.07.001
14. Amini K, Akhbarizadeh A, Javadpour S (2012) Investigating the effect of holding duration on the microstructure of 1.2080 tool steel during the deep cryogenic heat treatment. Vacuum 86(10):1534–1540. https://doi.org/10.1016/j.vacuum.2012.02.013
15. Gill SS, Singh H, Singh R, Singh J (2011) Flank wear and machining performance of cryogenically treated tungsten carbide inserts. Mater Manuf Process 26(11):1430–1441. https://doi.org/10.1080/10426914.2011.557128
16. Özbek NA, Çiçek A, Gülesin M, Özbek O (2014) Investigation of the effects of cryogenic treatment applied at different holding times to cemented carbide inserts on tool wear. Int J Mach Tools Manuf 86:34–43. https://doi.org/10.1016/j.ijmachtools.2014.06.007
17. Yong J, Ding C (2011) Effect of cryogenic treatment on WC–Co cemented carbides. Mater Sci Eng A 528(3):1735–1739. https://doi.org/10.1016/j.msea.2010.11.009
18. Gill SS, Singh J, Singh H, Singh R (2011) Investigation on wear behaviour of cryogenically treated TiAlN coated tungsten carbide inserts in turning. Int J Mach Tools Manuf 51(1):25–33. https://doi.org/10.1016/j.ijmachtools.2010.10.003
19. Thakur DG, Ramamoorthy B, Vijayaraghavan L (2014) Effect of posttreatments on the performance of tungsten carbide (K20) tool while machining (turning) of Inconel 718. Int J Adv Manuf Technol 76(1–4):587–596. https://doi.org/10.1007/s00170-014-6279-4
20. SreeramaReddy TV, Sornakumar T, VenkataramaReddy M, Venkatram R (2009) Machinability of C45 steel with deep cryogenic treated tungsten carbide cutting tool inserts. Int J Refract Met Hard Mater 27(1):181–185. https://doi.org/10.1016/j.ijrmhm.2008.04.007
21. Özbek NA, Çiçek A, Gülesin M, Özbek O (2016) Effect of cutting conditions on wear performance of cryogenically treated tungsten carbide inserts in dry turning of stainless steel. Tribol Int 94:223–233. https://doi.org/10.1016/j.triboint.2015.08.024
22. Vadivel K, Rudramoorthy R (2008) Performance analysis of cryogenically treated coated carbide inserts. Int J Adv Manuf Technol 42(3–4):222–232. https://doi.org/10.1007/s00170-008-1597-z
23. Gill SS, Singh J, Singh H, Singh R (2011) Metallurgical and mechanical characteristics of cryogenically treated tungsten carbide (WC–Co). Int J Adv Manuf Technol 58(1–4):119–131. https://doi.org/10.1007/s00170-011-3369-4
24. Saito H, Iwabuchi A, Shimizu T (2006) Effects of Co content and WC grain size on wear of WC cemented carbide. Wear 261(2):126–132. https://doi.org/10.1016/j.wear.2005.09.034
25. Bonny K, De Baets P, Perez Y, Vleugels J, Lauwers B (2010) Friction and wear characteristics of WC–Co cemented carbides in dry reciprocating sliding contact. Wear 268(11–12):1504–1517. https://doi.org/10.1016/j.wear.2010.02.029
26. Kagnaya T, Boher C, Lambert L, Lazard M, Cutard T (2009) Wear mechanisms of WC–Co cutting tools from high-speed tribological tests. Wear 267(5–8):890–897. https://doi.org/10.1016/j.wear.2008.12.035
27. Menezes PL, Nosonovsky M, Kailas SV, Lovell MR (2013) Friction and wear. In: Menezes PL, Nosonovsky M, Ingole SP, Kailas SV, Lovell MR (eds) Tribology for scientists and engineers. Springer, New York, pp 43–91. https://doi.org/10.1007/978-1-4614-1945-7_2
28. Li A, Zhao J, Luo H, Pei Z, Wang Z (2011) Progressive tool failure in high-speed dry milling of Ti-6Al-4V alloy with coated carbide tools. Int J Adv Manuf Technol 58(5–8):465–478. https://doi.org/10.1007/s00170-011-3408-1
29. Khanna N, Davim JP (2015) Design-of-experiments application in machining titanium alloys for aerospace structural components. Measurement 61:280–290. https://doi.org/10.1016/j.measurement.2014.10.059
30. Zhang S, Li JF, Sun J, Jiang F (2009) Tool wear and cutting forces variation in high-speed end-milling Ti-6Al-4V alloy. Int J Adv Manuf Technol 46(1–4):69–78. https://doi.org/10.1007/s00170-009-2077-9
31. Sun Y, Sun J, Li J, Li W, Feng B (2013) Modeling of cutting force under the tool flank wear effect in end milling Ti6Al4V with solid carbide tool. Int J Adv Manuf Technol 69(9–12):2545–2553. https://doi.org/10.1007/s00170-013-5228-y
32. Ítalo Sette Antonialli A, Eduardo Diniz A, Pederiva R (2010) Vibration analysis of cutting force in titanium alloy milling. Int J Mach Tools Manuf 50(1):65–74. https://doi.org/10.1016/j.ijmachtools.2009.09.006
33. Nouari M, Makich H (2014) Analysis of physical cutting mechanisms and their effects on the tool wear and chip formation process when machining aeronautical titanium alloys: Ti-6Al-4V and Ti-55531. In: Davim JP (ed) Machining of titanium alloys. Springer, New York, pp 79–111
34. Yuan SM, Yan LT, Liu WD, Liu Q (2011) Effects of cooling air temperature on cryogenic machining of Ti–6Al–4V alloy. J Mater Process Technol 211(3):356–362. https://doi.org/10.1016/j.jmatprotec.2010.10.009
35. Strano M, Albertelli P, Chiappini E, Tirelli S (2015) Wear behaviour of PVD coated and cryogenically treated tools for Ti-6Al-4V turning. Int J Mater Form 8(4):601–611. https://doi.org/10.1007/s12289-014-1215-6

36. Mo JL, Zhu MH, Leyland A, Matthews A (2013) Impact wear and abrasion resistance of CrN, AlCrN and AlTiN PVD coatings. Surf Coat Technol 215:170–177. https://doi.org/10.1016/j.surfcoat.2012.08.077
37. Aykut Ş, Bagci E, Kentli A, Yazıcıoğlu O (2007) Experimental observation of tool wear, cutting forces and chip morphology in face milling of cobalt based super-alloy with physical vapour deposition coated and uncoated tool. Mater Des 28(6):1880–1888. https://doi.org/10.1016/j.matdes.2006.04.014
38. Wang CY, Xie YX, Qin Z, Lin HS, Yuan YH, Wang QM (2015) Wear and breakage of TiAlN- and TiSiN-coated carbide tools during high-speed milling of hardened steel. Wear 336-337:29–42. https://doi.org/10.1016/j.wear.2015.04.018
39. Kasim MS, Che Haron CH, Ghani JA, Sulaiman MA, Yazid MZA (2013) Wear mechanism and notch wear location prediction model in ball nose end milling of Inconel 718. Wear 302(1–2):1171–1179. https://doi.org/10.1016/j.wear.2012.12.040